

The first photometric study of the short period shallow contact system LO Comae

Y. Zhang,¹ Q. W. Han,^{2,3,4} and J. Z. Liu¹

ABSTRACT

In this paper, the first complete photometric light curves in the B , V , and R passbands for an eclipsing binary LO Com are presented, and the photometric solution for the LO Com is derived by analyzing these light curves by using the Wilson and Devinney code. From the photometric solution, it is found that the LO Com is a W-type W UMa binary with a mass ratio of $q = m_2/m_1 = 2.478$ and a contact degree of $f = (3.2 \pm 0.25)\%$. By combining the two new minimum times with those published earlier in the literature, we have found that the ($O-C$) curve shows a downward parabolic variation corresponding to a long-term decrease in the orbital period with a rate of $dP/dt = -1.18 \times 10^{-7} \text{ days yr}^{-1}$. This long-term decrease in its orbital period may be caused by mass transfer from the more massive component to the less massive one.

Subject headings: binaries: close — binaries: eclipsing — stars: evolution — stars: individual (LO Com)

1. Introduction

W Ursae Majoris (W UMa) binaries are eclipsing variables in which both components have filled their Roche lobes and shared a common envelope. As the most common observed variables, their eclipsing light curves have nearly equal depths. W UMa systems are important sources for testing the angular momentum evolution of binaries (Rucinski 2000). They

¹Xinjiang Astronomical Observatory, Chinese Academy of Sciences, Urumqi 830011, China; zhy@xao.ac.cn

²Yunnan Observatory, Chinese Academy of Sciences, Kunming 650011, China

³Key Laboratory for the Structure and Evolution of Celestial Objects, Chinese Academy of Sciences, Kunming 650011, China

⁴University of Chinese Academy of Sciences, Beijing 100049, China

have a high spatial frequency of occurrence and can also be used as standard candle for distance determinations (Rucinski 1997). They play an important role in studying the Galaxy structure. More importantly, the two components in W UMa systems transfer the mass and energy between themselves. They are good targets for understanding the energy and mass transfer mechanism (Li et al. 2004). On the other hand, they also play an important role in investigating the stellar evolution as they are the possible progenitors for some important objects, e.g. blue stragglers (Chen & Han 2008) and fast rotating stars (Jiang et al. 2013).

The majority of contact binary systems with short periods belong to W-subtype systems (Webbink 2003), and in this system the more massive component is the cooler one. Most of the W-subtype contact systems have shallow contact characteristics. Thus, they are the excellent objects for testing the thermal relaxation oscillation (TRO) model (Lucy 1976; Flannery 1976; Robertson & Eggleton 1977; Lucy & Wilson 1979; Li et al. 2004, 2005). In the TRO model, the W UMa binaries oscillate between contact and semi-detached states. In the semi-detached phase, the primary continues to fill its Roche lobe and the mass transfer from the primary to the secondary, whereas no energy transfers between them. In the contact phase, energy transfers from the primary to the secondary, and the mass transfers from the secondary to the primary. For the case that a W UMa binary has low shallow contact and keeps expanding, the contact configuration can break, and the system will evolve into the semi-detached state. Therefore, the short shallow contact systems are important targets to test the TRO theory.

The orbital periods of W UMa binaries are between 0.22 and 1.00 days (Gazeas & Niarchos 2006). The short-period W UMa binary LO Com (GSC 1991-1390, 2MASS J12320490+2622477, NSVS 7622465; $\alpha_{2000} = 12^{\text{h}}32^{\text{m}}04^{\text{s}}.91$, $\delta_{2000} = +26^{\circ}22'47''.7$) is classified as an EW-type eclipsing binary and is poorly investigated. Even though Blattler & Diethelm (2001) presented the light curves for this system, no complete photometric analysis has been published. In this paper, we show as the first time complete photometric or charge-coupled device (CCD) light curves in the B , V , and R passbands for the LO Com in Section 2. Then, the photometric solution with the Wilson and Devinney (W-D) program and analysis of the orbital period are presented in Sections 3 and 4, respectively. Finally, the discussions based on the photometric solution and orbital period variation are presented in Section 5.

2. Observations

CCD observations of the LO Com were taken on 2015 March 21 and 25 at the Nanshan 1.0 m telescope of Xinjiang Astronomical Observatory. The telescope is equipped with a 4K \times 4K camera CCD. During the observation, the Johnson-Cousins BVR filters were used.

The images were reduced with the aperture photometry package of IRAF.¹ Figure 1 shows one of the observed CCD images containing the variable stars, the comparison star, and the check star. Table 1 presents the coordinates of the variable, comparison, and check stars. Our observation data of three passbands are listed in Table 6, in delta magnitudes, the variable star minus the comparison star.

The complete light curves in the BVR passbands are presented in the top panel of Figure 2. The orbital phases of these observations were obtained by $Min.I = 2457107.2343 + 0^d.2863601 \times E$, where the 2457107.2343 is one of the new times of light minima obtained by us and the period is adopted from Blattler & Diethelm (2001). The magnitude differences between the comparison and check stars in the BVR passbands are shown in the bottom panel of Figure 2; the bottom panel shows the authenticity of the variations of the light curves for the target. The standard observation accuracies are about 0.021, 0.016, and 0.011 for the $B, V,$ and R bands, respectively. From Figure 2, it can be seen that the light curves are typically the EW-type, which are symmetric in all passbands and have no O’Connell effects (different heights of the two light maxima). Figure 2 also shows that there is ~ 0.13 mag for three passbands between the depths of the two minima. From the observations, two times of the minimum light were derived for each passband by using the method of Kwee & van Woerden (1956) listed in Table 2.

3. Photometric solution for the LO Com

The light curves shown in Figure 2 are symmetric and complete, all these are very useful for determining a reliable photometric solution for the LO Com. In order to derive

¹IRAF is distributed by the National Optical Astronomy Observatory, which is operated by the Association of Universities for Research in Astronomy, Inc., under the cooperative agreement with the National Science Foundation.

Table 1. The coordinates of the variable, Comparison, and Check stars

Objects	Name	R.A.(2000)	DEC.(2000)	B	$(B - R)$
Variable	LO Com	12:32:04.91	+26:22:47.7	14.0	1.5
Comparison	Arty 804	12:31:52.80	+26:24:23.7	14.3	1.4
Check	2MASS J12314932+2620407	12:31:49.32	+26:20:40.7	15.4	1.2

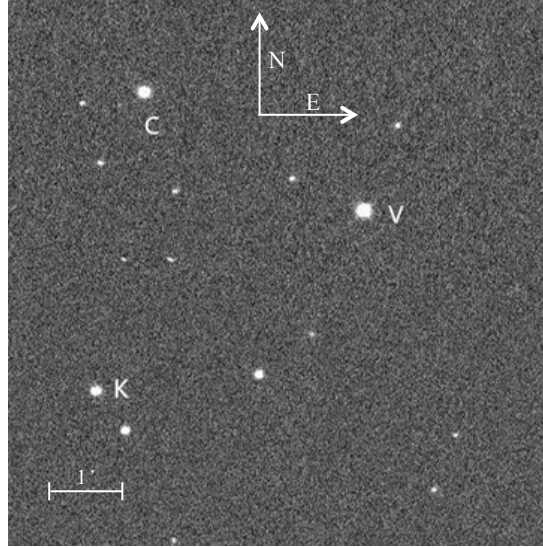


Fig. 1.— A CCD image of the LO Com V, C, K indicate the variable, comparison, and check stars, respectively.

Table 2. New times of light minimum of the LO Com.

HJD	Error	Type	Filter
2457107.2343	0.0001	I	B
2457107.2344	0.0002	I	V
2457107.2342	0.0001	I	R
2457103.3682	0.0003	II	B
2457103.3682	0.0002	II	V
2457103.3684	0.0001	II	R

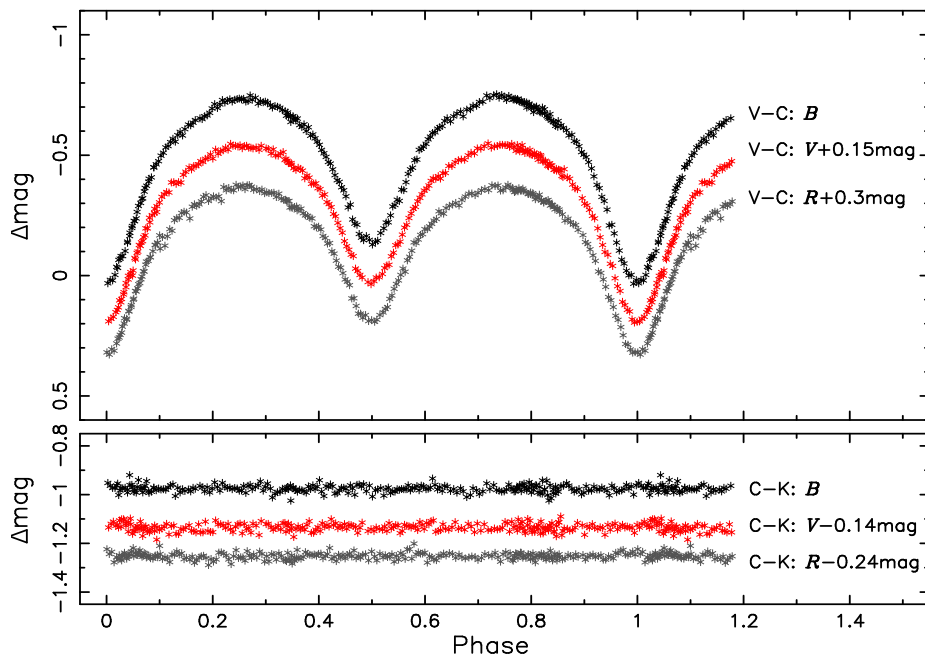


Fig. 2.— Top panel shows the CCD photometric light curves in the BVR passbands for the LO Com. The black, red, and gray asterisks indicate for the B , V and R passbands, respectively. Note that the curve in the V and R passbands are shifted by $+0.15$ and $+0.30$ mag, respectively. In the bottom panel, the magnitude differences between the comparison and check stars are shown. Here, shifts of -0.14 and -0.24 mag are also made for the V and R passbands, respectively.

Table 3. Assumed parameters during Photometric solution

Parameters	Values
$g_1 = g_2$	0.32
$A_1 = A_2$	0.5
$x_{1bolo} = x_{2bolo}$	0.082
$y_{1bolo} = y_{2bolo}$	0.646
$x_{1B} = x_{2B}$	0.778
$y_{1B} = y_{2B}$	0.301
$x_{1V} = x_{2V}$	0.680
$y_{1V} = y_{2V}$	0.297
$x_{1R} = x_{2R}$	0.582
$y_{1R} = Y_{2R}$	0.295
T1	5178 K

Table 4. Photometric solution of the LO Com

Parameters	Values
$i(^{\circ})$	79.991 ± 0.097
$\Omega_1 = \Omega_2$	5.8630 ± 0.0033
$T_2(\text{K})$	4874 ± 3
$q(M_2/M_1)$	2.478 ± 0.012
$L_1/(L_1 + L_2)_B$	0.4069 ± 0.0052
$L_1/(L_1 + L_2)_V$	0.3842 ± 0.0039
$L_1/(L_1 + L_2)_R$	0.3669 ± 0.003
$r_1(\text{pole})$	0.2873 ± 0.0018
$r_1(\text{side})$	0.3002 ± 0.0022
$r_1(\text{back})$	0.3358 ± 0.0037
$r_2(\text{pole})$	0.4385 ± 0.0016
$r_2(\text{side})$	0.4694 ± 0.0021
$r_2(\text{back})$	0.4986 ± 0.0028
$f_{over}(\%)$	3.2 ± 0.25
$\sum W(O - C)^2$	0.000259

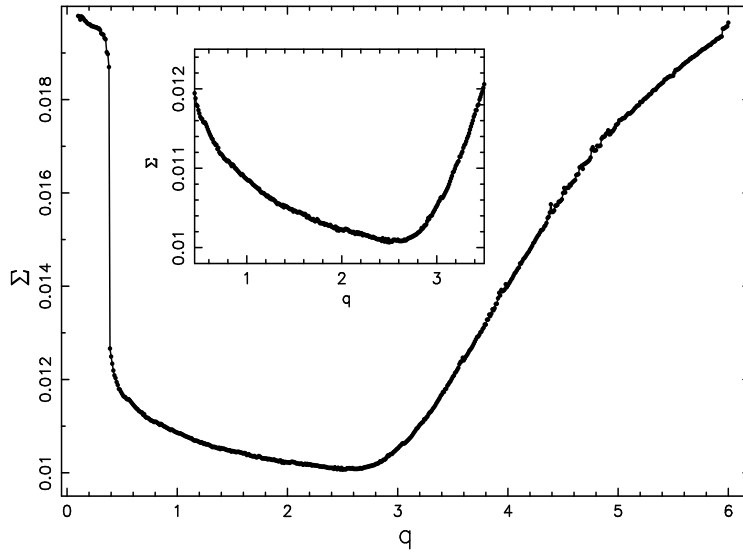


Fig. 3.— Relation between $\Sigma W(O - C)^2$ and q of the LO Com.

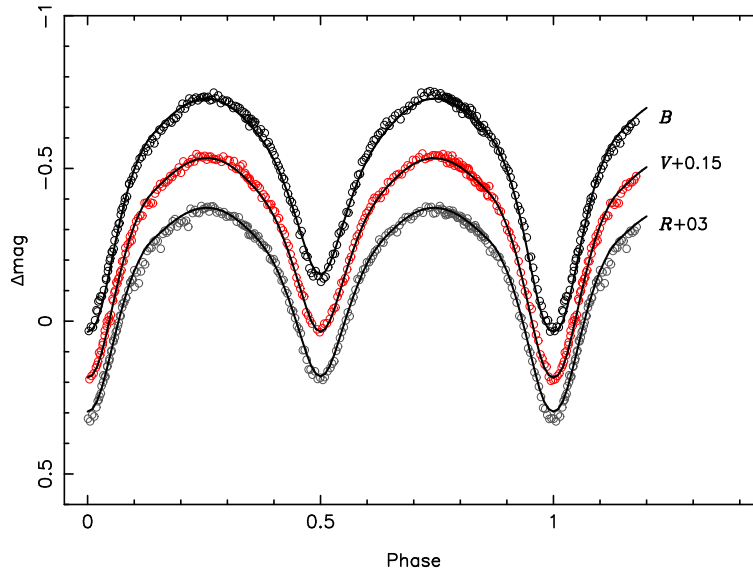


Fig. 4.— Observations (open circles) and computed (solid lines) light curves based on the W-D method for the B , V , and R passbands. Note that the magnitudes and curves in the V and R passbands are shifted by $+0.15$ and $+0.3$ mag, respectively.

the photometric parameters of the LO Com, the 2010 version of the W-D program (Wilson & Devinney 1971; Wilson 1979, 1990; Van Hamme & Wilson 2007; Wilson 2008) has been adopted. The spectroscopic observation can offer a reliable mass ratio. Since this system is relatively faint, minimal information about its radial velocity is available. We thus adopted thus only photometric data in our analyses. During the procedure of modeling the photometry, the effective temperature of star 1 (the star eclipsed at the primary light minimum) should be specified. Since the light curve only offers constraints on the temperature ratio by using the depth of eclipses, rather than constraints on the temperature, we estimated the temperature of star 1 based on $(J - H)$ color by the expression (Collier Cameron et al. 2007)

$$T_{\text{eff}} = -4369.5(J-H) + 7188.2 \quad (4000K < T_{\text{eff}} < 7000K), \quad (1)$$

where J and H magnitudes are obtained from the 2MASS All-Sky Catalog of point sources (Cutri et al. 2003). From Equation (1), the effective temperature T_1 of the hotter component in the LO Com is derived to be of 5178 K. This suggests that the LO Com is a late-type W UMa system with a convective envelope, implying that the gravity-darkening coefficients $g_1 = g_2 = 0.32$ (Lucy 1967) and the bolometric albedos $A_1 = A_2 = 0.5$ (Ruciński 1969). Note that the W-D program itself can automatically calculate the bolometric and passband limb-darkening coefficients taken from van Hamme (1993), and we choose the logarithmic functions (listed in Table 3). The adjusted parameters are: the orbital inclination i , the temperature of star 2 T_2 , the dimensionless surface potential Ω_1 and Ω_2 , and the monochromatic luminosities of star 1 L_{1B} , L_{1V} and L_{1R} .

Since so far no photometric and spectroscopic solutions have been published for the LO Com, it was necessary to obtain an accurate photometric solution for it. A series of fixed values of the mass ratio q in the range of 0.1–6.0 by step of 0.01 were used. For each assumed mass ratio, different models (detached, semi-detached, contact, near-contact models) were tested, and the solutions usually converged to the model 3 (a contact configuration) during the computation. Therefore, a series of the sum of the weighted squared residuals, $\Sigma W(O - C)^2$ (hereafter Σ), were obtained. The relation between the resulting Σ and the assumed q is shown in Figure 3. It can be seen that the Σ has a minimum value at $q = 2.5$. Then, we chose 2.5 as the initial value of q and took it as an adjustable parameter in subsequent calculations until a convergent solution was obtained. Finally, q was convergent to 2.478. The parameters of the final photometric solution are listed in Table 4.

The theoretical light curves also have been obtained with the light curve program. The theoretical light curves (solid lines) together with the observations (open circles) are plotted in Figure 4. It can be seen that the theoretical light curves fit to the observed data very well. Figure 5 also shows the geometrical structure at four (0.00, 0.25, 0.50, and 0.75) different

orbital phases. The photometric solution shows that the LO Com has a lower contact degree of $f = 3.2\%$.

For the case of poor spectroscopic data about the LO Com, we estimated the absolute parameters by the $J - H$ color. The $J - H$ color indicates that the spectral type of the LO Com is K0; its mass can be estimated to be $M_2 = 0.79 M_\odot$ (Cox 2000). Then, based on the mass ratio $q = 2.478$, the mass of the primary component can be estimated as approximately $M_1 = 0.32 M_\odot$.

4. Orbital period variation for the LO Com

The orbital period change is one of the observational properties of binary stars. The study of the orbital period change for the LO Com is absent in the literature. For investigating this property, we collect the light minimum times from eclipsing binary minima database (O-C) Gateway.² Among these minimum times, only two are visual observations, and we reject these visual observations and select only the photoelectric or CCD observations. Including our new minimum times, a total number of 49 minimum times were obtained, and the period spans over 15 years (listed in Table 5). Based on one of our primary times of light minimum (2457107.2343) and the period 0.2863601 given by Blattler & Diethelm (2001), a new corrected linear ephemeris was obtained:

$$Min.I = 2457107.23766(4) + 0.28636058(3) \times E \quad (2)$$

The $(O - C)$ values are obtained based on this new linear ephemeris, and the relevant $(O - C)$ diagram is shown in the upper panel of Figure 6. A long-term period decrease can be seen clearly. At first, the $(O - C)$ data were fitted by a parabola; the fitted result is

$$Min.I = 2457107.23717(\pm 0.00088) + 0.28636003(\pm 0.00000019) \times E - 5.342(\pm 0.5) \times 10^{-11} \times E^2. \quad (3)$$

In the top panel of Figure 6, the red dashed line shows the fitted parabola. Equation (3) implies that the orbital period of the LO Com decreases secularly at a rate of $dP/dt = -1.18 \times 10^{-7} \text{days yr}^{-1}$.

²<http://var.astro.cz/ocgate/>

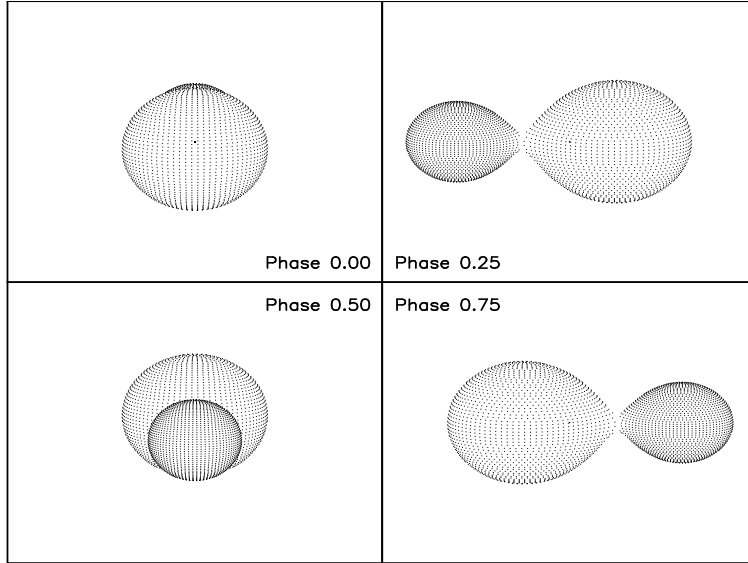


Fig. 5.— Configurations at the phases 0.00, 0.25, 0.50, and 0.75.

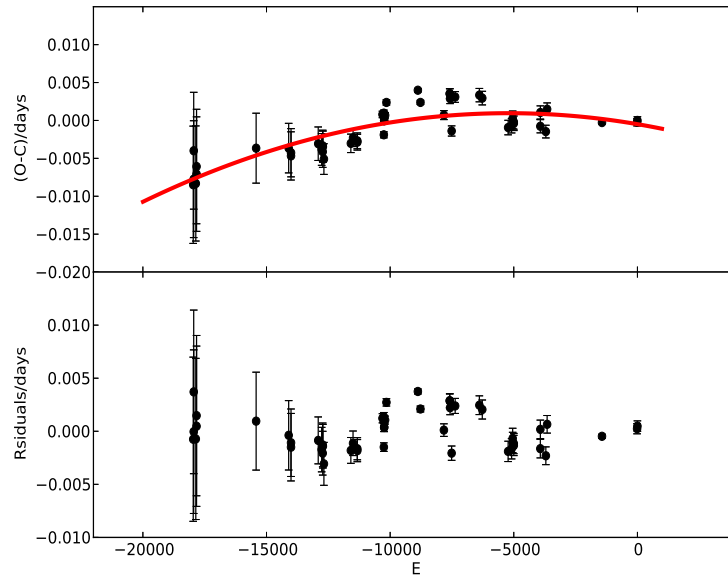


Fig. 6.— Upper: The $(O - C)$ diagram for all minimum times of the LO Com. The dots are obtained by the linear ephemeris in Equation (2), whereas the red solid line indicates a long-term decrease. Here the red solid line indicates a cyclic variation. The residuals after the subtraction of the best fit (the red solid line in the upper panel) are displayed in the bottom panel.

Table 5. The CCD Times of Minimum Light of the Lo Com

HJD+240 0000	Error	Min.	HJD+240 0000	Error	Min.	HJD+240 0000	Error	Min.
51962.90980	0.0001	s	53813.80450	0.0001	p	54955.66630	0.0011	s
51968.49456	0.0023	p	53863.34440	0.0003	p	54996.47710	0.0007	s
51968.64149	0.0023	s	53863.48740	0.0015	s	55276.68070	0.0013	p
51992.83460	0.0001	p	54154.57610	0.0008	s	55310.47080	0.0025	p
52001.42664	0.0022	p	54170.46640	0.0005	s	55609.85640	0.0005	p
52001.57082	0.0025	s	54170.61198	0.0001	s	55650.37660	0.0003	s
52691.55790	0.0017	p	54170.61244	0.0005	s	55662.40470	0.0004	p
53068.40780	0.0013	p	54174.47730	0.0001	s	55662.54750	0.0007	p
53095.46780	0.0015	s	54174.62050	0.0027	p	55675.43360	0.0016	p
53095.61140	0.0003	p	54185.35970	0.0005	p	55675.57660	0.0006	s
53410.60870	0.0005	p	54200.39530	0.0010	s	55982.84060	0.0004	s
53450.41200	0.0004	p	54564.36060	0.0004	s	55982.98560	0.0007	s
53462.43960	0.0017	p	54594.42680	0.0006	s	56046.69820	0.0003	s
53462.58200	0.0010	s	54865.89450	0.0005	s	56061.44870	0.0020	s
53464.44400	0.0030	p	54933.47830	0.0007	s	56696.88000	0.0003	p
53476.46950	0.0011	p	54933.62150	0.0003	p	57103.36820	0.0002	s
53788.46090	0.0011	s	54937.48670	0.0009	s	57107.23430	0.0002	p

5. Discussions and conclusions

In this paper, the first complete photometric light curves of the B , V and R passbands were presented. The photometric solution indicates that the LO Com is a W-type W UMa binary system with a contact degree of $f = (3.2 \pm 0.25)\%$. The orbital period variations were also studied, and a secular decrease in its orbital period has been found. The orbital period decreases with a rate of $dP/dt = -1.18 \times 10^{-7}$ days yr^{-1} .

The long-term decrease of the orbital period of the LO Com may be caused by angular momentum loss (AML) due to the magnetic stellar wind. According to the formula given by Guinan & Bradstreet (1988):

$$\left(\frac{dP}{dt}\right)_{\text{AML}} \approx -1.1 \times 10^{-8} q'^{-1} (1 + q')^2 (M_1 + M_2)^{-\frac{5}{3}} k^2 \times (M_1 R_1^4 + M_2 R_2^4) P^{-\frac{7}{3}}, \quad (4)$$

the decreasing rate of the period can be estimated as $dP/dt_{(\text{AML})} = -4.92 \times 10^{-8}$ days yr^{-1} . Here, the M_1 , M_2 , R_1 , and R_2 in Equation (4) are the masses and radii of two components in solar units, respectively. Note that the mass ratio $q' = 1/q = M_1/M_2 < 1.0$; the k^2 was set to be 0.1.

The result given above seems to imply that the AML can explain the long-term period decrease for the LO Com. However, the long-term period decrease of the LO Com might also be caused by the mass transfer from the more massive component to the less massive one by the well-known equation

$$\frac{\dot{P}}{P} = 3\dot{M}_2 \left(\frac{1}{M_1} - \frac{1}{M_2} \right). \quad (5)$$

Therefore, the mass transfer rate can be estimated as $dM_2/dt = -0.9 \times 10^{-7} M_\odot \text{yr}^{-1}$. The minus sign indicates that the more massive component loses its mass. Then, the time scale of the mass transfer can be estimated to be as approximately 8.7×10^6 yr. The thermal time scale of the massive component can be estimated as $\tau_{th} \sim GM_2/R_2L_2 \sim 2.8 \times 10^7$ yr (Paczynski 1971), which is longer than the mass transfer duration. This implies that the primary component cannot stay in the thermal equilibrium and the mass transfer in the LO Com is unstable.

However, a comprehensive understanding of orbital period variation for the LO Com comes from the coupled contributions of the results of mass transfer from the more massive component to the less massive one, and the AML is due to magnetic stellar winds. Although, the contribution of AML is a minor aspect ($[-4.92 \times 10^{-8} / -1.18 \times 10^{-7}] < 50\%$) for the interpretation of this long-term decrease tendency. We need to note that the presence of

the AML in LO Com may play an important role for the evolutionary stages from initially detached binary into overcontact binary systems (e.g., Mestel 1968; vant Veer 1979; Vilhu 1982; Eggen & Iben 1989) for the shallow contact degree ($f = (3.2 \pm 0.25)$) shown in this paper. Meanwhile, we can also see that the time scale of the secular decrease trend is about $T_P \sim P/(dP/dt) \sim 2.4 \times 10^6 \text{yr}$, which is close to the time scale of the mass transfer $\sim 8.7 \times 10^6 \text{yr}$. This indicates that the long-term decrease in the orbital period of LO Com may be caused by the thermally conservative mass transfer from the more massive component to the less massive one.

From the photometric solution, it has been found that the LO Com is a shallow contact binary system with a contact degree of $f = 3.2\%$. The temperature of the primary is hotter by about 304 K than the secondary component. This indicates that this binary system could be in a very important evolution phase of the TRO (Flannery 1976; Eggleton 1996; Csizmadia & Klagyivik 2004; Li et al. 2004, 2005, 2008). The binary system LO Com might be at the beginning of the duration that the full energy transfer is lost, which is indicated by the observed properties (large temperature difference and unstable mass transfer). When the effective energy transfer is lost, the secondary contracts rapidly, and the mass transfers from the primary component to the secondary component. Therefore, the secondary might have a higher temperature than the primary due to the gravitational energy transformed to thermal energy for the secondary, and rapid expansion could lead to the expense of the primary. The mass transfer rate might reach the highest value in a cycle and could induce the dynamically instability of the mass transfer (Li et al. 2004).

In summary, the LO Com is a short-period shallow contact binary system. While the complete photometric light curves are presented, long-time monitoring observations (especially spectroscopic observations) are still necessary to offer more information about this system.

We thank the anonymous referee for very valuable comments that helped us to improve the manuscript. This work is partially supported by the program of the Light in China' Western Region (LCWR, grant No. 2015-XBQN-A-02), the National Natural Science Foundation of China (grant No. 11303080), and Youth Innovation Promotion Association CAS. The CCD photometric data of LO Com were observed with the Nanshan 1.0 m telescope of Xinjiang Astronomical Observatory.

REFERENCES

Blattler, E., & Diethelm, R. 2001, Information Bulletin on Variable Stars, 5052, 1

- Chen, X., & Han, Z. 2008, MNRAS, 384, 1263
- Collier Cameron, A., et al. 2007, MNRAS, 380, 1230
- Cox, A. N. 2000, Introduction, ed. A. N. Cox, 1
- Csizmadia, S., & Klagyivik, P. 2004, A&A, 426, 1001
- Cutri, R. M., et al. 2003, VizieR Online Data Catalog, 2246, 0
- Eggen, O. J., & Iben, Jr., I. 1989, AJ, 97, 431
- Eggleton, P. P. 1996, in *Astronomical Society of the Pacific Conference Series*, Vol. 90, *The Origins, Evolution, and Destinies of Binary Stars in Clusters*, ed. E. F. Milone & J.-C. Mermilliod, 257
- Flannery, B. P. 1976, ApJ, 205, 217
- Gazeas, K. D., & Niarchos, P. G. 2006, MNRAS, 370, L29
- Guinan, E. F., & Bradstreet, D. H. 1988, in *NATO Advanced Science Institutes (ASI) Series C*, Vol. 241, *NATO Advanced Science Institutes (ASI) Series C*, ed. A. K. Dupree & M. T. V. T. Lago, 345
- Jiang, D., Han, Z., Yang, L., & Li, L. 2013, MNRAS, 428, 1218
- Kwee, K. K., & van Woerden, H. 1956, *Bull. Astron. Inst. Netherlands*, 12, 327
- Li, L., Han, Z., & Zhang, F. 2004, MNRAS, 351, 137
- . 2005, MNRAS, 360, 272
- Li, L., Zhang, F., Han, Z., Jiang, D., & Jiang, T. 2008, MNRAS, 387, 97
- Lucy, L. B. 1967, ZAp, 65, 89
- . 1976, ApJ, 205, 208
- Lucy, L. B., & Wilson, R. E. 1979, ApJ, 231, 502
- Mestel, L. 1968, MNRAS, 138, 359
- Paczyński, B. 1971, ARA&A, 9, 183
- Robertson, J. A., & Eggleton, P. P. 1977, MNRAS, 179, 359

Ruciński, S. M. 1969, *Acta Astron.*, 19, 245

Rucinski, S. M. 1997, *AJ*, 113, 407

—. 2000, *AJ*, 120, 319

van Hamme, W. 1993, *AJ*, 106, 2096

Van Hamme, W., & Wilson, R. E. 2007, *ApJ*, 661, 1129

vant Veer, F. 1979, *A&A*, 80, 287

Vilhu, O. 1982, *A&A*, 109, 17

Webbink, R. F. 2003, in *Astronomical Society of the Pacific Conference Series*, Vol. 293, 3D
Stellar Evolution, ed. S. Turcotte, S. C. Keller, & R. M. Cavallo, 76

Wilson, R. E. 1979, *ApJ*, 234, 1054

—. 1990, *ApJ*, 356, 613

—. 2008, *ApJ*, 672, 575

Wilson, R. E., & Devinney, E. J. 1971, *ApJ*, 166, 605

A. The observation data of LO Com

Table 6. the original photometric Data of LO Com in the B , V , and R passbands.

HJD 2457,100+	$\Delta m(B)$	HJD 2457,100+	$\Delta m(B)$	HJD 2457,100+	$\Delta m(B)$	HJD 2457,100+	$\Delta m(B)$
3.2307	-0.036	3.3832	-0.310	3.4687	-0.618	7.2534	-0.319
3.2318	-0.065	3.3844	-0.357	7.1678	-0.731	7.2547	-0.349
3.2331	-0.081	3.3856	-0.355	7.1691	-0.728	7.2560	-0.373
3.2366	-0.141	3.3868	-0.388	7.1704	-0.726	7.2572	-0.402
3.2377	-0.164	3.3880	-0.422	7.1717	-0.728	7.2585	-0.408
3.2389	-0.198	3.3892	-0.441	7.1731	-0.714	7.2598	-0.450
3.2401	-0.227	3.3904	-0.448	7.1745	-0.719	7.2611	-0.462
3.2413	-0.237	3.3915	-0.479	7.1759	-0.714	7.2624	-0.475
3.2425	-0.289	3.3927	-0.482	7.1772	-0.704	7.2637	-0.498
3.2437	-0.302	3.3939	-0.522	7.1784	-0.700	7.2650	-0.510
3.2448	-0.321	3.3950	-0.527	7.1799	-0.702	7.2663	-0.532
3.2460	-0.364	3.3962	-0.535	7.1816	-0.683	7.2675	-0.538
3.2480	-0.390	3.3976	-0.547	7.1830	-0.675	7.2688	-0.554
3.2508	-0.449	3.3988	-0.566	7.1842	-0.675	7.2701	-0.568
3.3223	-0.664	3.3999	-0.577	7.1859	-0.657	7.2714	-0.556
3.3235	-0.661	3.4011	-0.592	7.1872	-0.671	7.2727	-0.583
3.3247	-0.638	3.4024	-0.595	7.1890	-0.640	7.2740	-0.597
3.3259	-0.662	3.4038	-0.610	7.1903	-0.633	7.2753	-0.582
3.3271	-0.654	3.4050	-0.616	7.1916	-0.642	7.2766	-0.608
3.3282	-0.652	3.4063	-0.621	7.1931	-0.624	7.2785	-0.627
3.3294	-0.625	3.4077	-0.642	7.1944	-0.613	7.2797	-0.624
3.3306	-0.617	3.4090	-0.653	7.1961	-0.603	7.2810	-0.635
3.3318	-0.628	3.4108	-0.640	7.1974	-0.582	7.2822	-0.646
3.3330	-0.600	3.4125	-0.661	7.1989	-0.585	7.2847	-0.653
3.3342	-0.616	3.4143	-0.673	7.2002	-0.559	7.2859	-0.650
3.3353	-0.581	3.4162	-0.681	7.2015	-0.555	7.2872	-0.662
3.3366	-0.586	3.4176	-0.661	7.2028	-0.537	7.2886	-0.665
3.3377	-0.570	3.4196	-0.689	7.2041	-0.513	7.2899	-0.676
3.3389	-0.556	3.4216	-0.691	7.2054	-0.502	7.2913	-0.694
3.3401	-0.543	3.4229	-0.705	7.2067	-0.492	7.2926	-0.712

Table 6—Continued

HJD 2457,100+	$\Delta m(B)$	HJD 2457,100+	$\Delta m(B)$	HJD 2457,100+	$\Delta m(B)$	HJD 2457,100+	$\Delta m(B)$
3.3413	-0.522	3.4249	-0.705	7.2080	-0.471	7.2941	-0.696
3.3425	-0.508	3.4264	-0.721	7.2095	-0.445	7.2955	-0.711
3.3437	-0.493	3.4283	-0.722	7.2108	-0.412	7.2968	-0.729
3.3449	-0.472	3.4303	-0.748	7.2125	-0.377	7.2982	-0.719
3.3460	-0.465	3.4320	-0.737	7.2138	-0.363	7.2995	-0.727
HJD 2457,100+	$\Delta m(V)$	HJD 2457,100+	$\Delta m(V)$	HJD 2457,100+	$\Delta m(V)$	HJD 2457,100+	$\Delta m(V)$
3.2311	-0.007	3.3812	-0.276	3.4679	-0.593	7.2525	-0.273
3.2322	-0.047	3.3824	-0.279	3.4691	-0.590	7.2538	-0.293
3.2334	-0.053	3.3836	-0.291	3.4703	-0.587	7.2551	-0.317
3.2346	-0.081	3.3848	-0.320	3.4714	-0.559	7.2564	-0.346
3.2358	-0.119	3.3860	-0.349	7.1695	-0.692	7.2577	-0.371
3.2370	-0.134	3.3872	-0.361	7.1708	-0.666	7.2589	-0.401
3.2381	-0.153	3.3884	-0.389	7.1721	-0.692	7.2603	-0.427
3.2393	-0.150	3.3896	-0.408	7.1736	-0.659	7.2615	-0.438
3.2405	-0.223	3.3907	-0.427	7.1750	-0.662	7.2628	-0.454
3.2417	-0.244	3.3919	-0.435	7.1763	-0.654	7.2641	-0.477
3.2429	-0.277	3.3931	-0.458	7.1776	-0.653	7.2654	-0.488
3.2441	-0.288	3.3943	-0.473	7.1789	-0.648	7.2667	-0.497
3.2453	-0.310	3.3954	-0.487	7.1808	-0.631	7.2680	-0.495
3.2464	-0.346	3.3966	-0.503	7.1821	-0.650	7.2693	-0.537
3.2484	-0.390	3.3980	-0.511	7.1834	-0.627	7.2706	-0.538
3.2512	-0.409	3.3992	-0.524	7.1847	-0.623	7.2718	-0.531
3.2524	-0.414	3.4003	-0.543	7.1863	-0.604	7.2731	-0.538
3.3215	-0.630	3.4015	-0.554	7.1876	-0.608	7.2745	-0.536
3.3227	-0.627	3.4028	-0.552	7.1894	-0.589	7.2757	-0.568
3.3239	-0.618	3.4042	-0.563	7.1907	-0.586	7.2770	-0.581
3.3251	-0.610	3.4054	-0.553	7.1920	-0.588	7.2789	-0.599
3.3263	-0.596	3.4067	-0.575	7.1935	-0.564	7.2801	-0.591
3.3274	-0.589	3.4081	-0.576	7.1948	-0.592	7.2814	-0.605

Table 6—Continued

HJD 2457,100+	$\Delta m(V)$	HJD 2457,100+	$\Delta m(V)$	HJD 2457,100+	$\Delta m(V)$	HJD 2457,100+	$\Delta m(V)$
3.3286	-0.598	3.4099	-0.605	7.1965	-0.558	7.2826	-0.605
3.3298	-0.593	3.4116	-0.605	7.1978	-0.552	7.2839	-0.612
3.3310	-0.586	3.4133	-0.621	7.1994	-0.528	7.2851	-0.625
3.3322	-0.554	3.4151	-0.629	7.2007	-0.512	7.2863	-0.622
3.3334	-0.565	3.4166	-0.632	7.2019	-0.509	7.2876	-0.635
3.3346	-0.557	3.4184	-0.631	7.2045	-0.471	7.2890	-0.639
3.3358	-0.531	3.4203	-0.649	7.2058	-0.449	7.2903	-0.653
3.3369	-0.532	3.4219	-0.660	7.2071	-0.442	7.2917	-0.636
3.3381	-0.533	3.4237	-0.657	7.2084	-0.423	7.2931	-0.673
3.3393	-0.513	3.4253	-0.678	7.2100	-0.398	7.2945	-0.656
3.3405	-0.509	3.4272	-0.677	7.2113	-0.387	7.2959	-0.666
3.3417	-0.482	3.4290	-0.687	7.2129	-0.346	7.2972	-0.670
3.3429	-0.487	3.4311	-0.699	7.2142	-0.309	7.2985	-0.681
3.3441	-0.455	3.4328	-0.681	7.2155	-0.277	7.2999	-0.673
3.3453	-0.447	3.4345	-0.686	7.2168	-0.248	7.3012	-0.697
3.3465	-0.434	3.4361	-0.688	7.2184	-0.236	7.3025	-0.689
3.3477	-0.406	3.4375	-0.693	7.2196	-0.199	7.3038	-0.689
3.3489	-0.396	3.4388	-0.693	7.2209	-0.190	7.3052	-0.686
3.3501	-0.369	3.4403	-0.692	7.2222	-0.139	7.3063	-0.691
3.3512	-0.347	3.4414	-0.692	7.2236	-0.106	7.3075	-0.679
3.3524	-0.328	3.4426	-0.685	7.2250	-0.086	7.3087	-0.688
3.3536	-0.293	3.4438	-0.697	7.2263	-0.041	7.3098	-0.689
3.3548	-0.272	3.4450	-0.682	7.2275	-0.027	7.3110	-0.681
3.3560	-0.257	3.4462	-0.668	7.2288	-0.008	7.3122	-0.681
3.3572	-0.237	3.4473	-0.673	7.2301	-0.001	7.3133	-0.678
3.3584	-0.231	3.4487	-0.680	7.2314	0.032	7.3150	-0.682
3.3596	-0.179	3.4500	-0.669	7.2327	0.045	7.3166	-0.672
3.3608	-0.169	3.4511	-0.672	7.2341	0.042	7.3177	-0.689
3.3619	-0.153	3.4524	-0.667	7.2354	0.040	7.3204	-0.678
3.3631	-0.142	3.4536	-0.672	7.2367	0.029	7.3216	-0.676

Table 6—Continued

HJD 2457,100+	$\Delta m(V)$	HJD 2457,100+	$\Delta m(V)$	HJD 2457,100+	$\Delta m(V)$	HJD 2457,100+	$\Delta m(V)$
3.3663	−0.123	3.4548	−0.651	7.2380	0.021	7.3231	−0.657
3.3679	−0.114	3.4560	−0.660	7.2393	0.002	7.3242	−0.674
3.3696	−0.127	3.4572	−0.653	7.2408	−0.018	7.3256	−0.649
3.3707	−0.142	3.4584	−0.651	7.2421	−0.039	7.3269	−0.648
3.3724	−0.143	3.4596	−0.644	7.2435	−0.072	7.3282	−0.657
3.3741	−0.157	3.4608	−0.623	7.2448	−0.102	7.3296	−0.663
3.3753	−0.181	3.4619	−0.627	7.2461	−0.149	7.3310	−0.635
3.3765	−0.192	3.4631	−0.607	7.2473	−0.164	7.3324	−0.619
3.3777	−0.195	3.4643	−0.616	7.2486	−0.171	7.3339	−0.617
3.3789	−0.230	3.4655	−0.607	7.2499	−0.217		
3.3800	−0.245	3.4667	−0.590	7.2512	−0.250		
HJD 2457,100+	$\Delta m(R)$	HJD 2457,100+	$\Delta m(R)$	HJD 2457,100+	$\Delta m(R)$	HJD 2457,100+	$\Delta m(R)$
3.2314	−0.038	3.3804	−0.245	3.4682	−0.579	7.2542	−0.318
3.2326	−0.054	3.3816	−0.265	3.4694	−0.574	7.2555	−0.345
3.2338	−0.088	3.3828	−0.280	7.1673	−0.655	7.2568	−0.361
3.2350	−0.123	3.3840	−0.303	7.1686	−0.650	7.2580	−0.376
3.2361	−0.121	3.3851	−0.329	7.1699	−0.650	7.2593	−0.401
3.2373	−0.153	3.3863	−0.316	7.1712	−0.653	7.2606	−0.427
3.2385	−0.170	3.3875	−0.363	7.1725	−0.661	7.2619	−0.436
3.2397	−0.200	3.3887	−0.378	7.1754	−0.639	7.2632	−0.412
3.2408	−0.236	3.3899	−0.403	7.1767	−0.638	7.2645	−0.460
3.2420	−0.247	3.3911	−0.438	7.1780	−0.635	7.2658	−0.424
3.2432	−0.269	3.3922	−0.435	7.1793	−0.617	7.2671	−0.463
3.2444	−0.296	3.3934	−0.450	7.1812	−0.623	7.2684	−0.493
3.2456	−0.317	3.3946	−0.469	7.1825	−0.613	7.2696	−0.486
3.2468	−0.358	3.3958	−0.472	7.1838	−0.603	7.2709	−0.530
3.2487	−0.377	3.3970	−0.493	7.1850	−0.610	7.2722	−0.539
3.2515	−0.427	3.3983	−0.493	7.1867	−0.606	7.2735	−0.540
3.2527	−0.437	3.3995	−0.504	7.1880	−0.594	7.2748	−0.560

Table 6—Continued

HJD 2457,100+	$\Delta m(R)$	HJD 2457,100+	$\Delta m(R)$	HJD 2457,100+	$\Delta m(R)$	HJD 2457,100+	$\Delta m(R)$
3.2539	-0.467	3.4007	-0.515	7.1898	-0.575	7.2761	-0.565
3.3218	-0.615	3.4019	-0.528	7.1911	-0.578	7.2774	-0.562
3.3230	-0.609	3.4032	-0.535	7.1924	-0.565	7.2792	-0.537
3.3242	-0.583	3.4045	-0.567	7.1939	-0.554	7.2805	-0.586
3.3254	-0.581	3.4057	-0.559	7.1952	-0.528	7.2817	-0.596
3.3266	-0.583	3.4071	-0.557	7.1969	-0.536	7.2829	-0.590
3.3278	-0.587	3.4084	-0.580	7.1982	-0.521	7.2843	-0.596
3.3290	-0.575	3.4102	-0.590	7.1997	-0.512	7.2854	-0.608
3.3302	-0.578	3.4119	-0.595	7.2010	-0.510	7.2866	-0.627
3.3314	-0.559	3.4136	-0.602	7.2023	-0.490	7.2880	-0.634
3.3326	-0.550	3.4154	-0.591	7.2036	-0.584	7.2893	-0.610
3.3337	-0.548	3.4169	-0.614	7.2049	-0.468	7.2907	-0.621
3.3349	-0.540	3.4188	-0.628	7.2062	-0.439	7.2920	-0.629
3.3361	-0.537	3.4207	-0.640	7.2075	-0.431	7.2935	-0.624
3.3373	-0.505	3.4223	-0.641	7.2088	-0.409	7.2949	-0.629
3.3385	-0.500	3.4241	-0.634	7.2103	-0.384	7.2962	-0.609
3.3397	-0.503	3.4256	-0.644	7.2116	-0.361	7.2975	-0.668
3.3409	-0.491	3.4275	-0.654	7.2133	-0.317	7.2989	-0.654
3.3420	-0.464	3.4293	-0.660	7.2146	-0.311	7.3002	-0.664
3.3433	-0.456	3.4314	-0.655	7.2159	-0.284	7.3015	-0.656
3.3445	-0.433	3.4331	-0.675	7.2172	-0.253	7.3028	-0.654
3.3456	-0.435	3.4348	-0.672	7.2187	-0.211	7.3042	-0.677
3.3468	-0.401	3.4364	-0.674	7.2200	-0.197	7.3055	-0.667
3.3480	-0.391	3.4378	-0.653	7.2213	-0.169	7.3067	-0.670
3.3492	-0.362	3.4391	-0.654	7.2226	-0.133	7.3078	-0.674
3.3504	-0.337	3.4406	-0.666	7.2239	-0.116	7.3090	-0.659
3.3516	-0.333	3.4418	-0.677	7.2253	-0.086	7.3102	-0.675
3.3528	-0.310	3.4430	-0.668	7.2266	-0.052	7.3113	-0.676
3.3540	-0.284	3.4442	-0.664	7.2279	-0.016	7.3125	-0.669
3.3552	-0.275	3.4453	-0.647	7.2292	-0.013	7.3137	-0.656

Table 6—Continued

HJD 2457,100+	$\Delta m(R)$	HJD 2457,100+	$\Delta m(R)$	HJD 2457,100+	$\Delta m(R)$	HJD 2457,100+	$\Delta m(R)$
3.3563	-0.260	3.4465	-0.657	7.2305	0.007	7.3153	-0.659
3.3575	-0.205	3.4477	-0.663	7.2318	0.020	7.3169	-0.651
3.3587	-0.206	3.4490	-0.653	7.2331	0.018	7.3181	-0.657
3.3599	-0.174	3.4503	-0.652	7.2345	0.019	7.3196	-0.642
3.3611	-0.142	3.4515	-0.647	7.2358	0.028	7.3207	-0.646
3.3623	-0.142	3.4528	-0.639	7.2371	0.006	7.3219	-0.643
3.3635	-0.125	3.4540	-0.645	7.2384	0.012	7.3234	-0.643
3.3650	-0.136	3.4552	-0.642	7.2397	-0.018	7.3246	-0.644
3.3666	-0.111	3.4564	-0.629	7.2411	-0.043	7.3259	-0.626
3.3683	-0.115	3.4575	-0.625	7.2424	-0.063	7.3272	-0.640
3.3699	-0.108	3.4587	-0.636	7.2439	-0.101	7.3286	-0.620
3.3711	-0.117	3.4599	-0.612	7.2451	-0.117	7.3299	-0.614
3.3727	-0.136	3.4611	-0.607	7.2464	-0.151	7.3314	-0.611
3.3744	-0.147	3.4623	-0.609	7.2477	-0.177	7.3327	-0.610
3.3756	-0.161	3.4635	-0.614	7.2490	-0.204	7.3342	-0.585
3.3768	-0.169	3.4647	-0.591	7.2503	-0.234	7.3357	-0.585
3.3780	-0.203	3.4658	-0.593	7.2516	-0.264	7.3371	-0.571
3.3792	-0.217	3.4670	-0.586	7.2529	-0.285		